Supplementary information
"Optomechanical thermal intermodulation noise"

S. A. Fedorov,* A. Beccari,* A. Arabmoheghi, N. J. Engelsen, and T. J. Kippenberg†
Institute of Physics (IPHYS), École Polytechnique Fédérale de Lausanne, 1015 Lausanne, Switzerland

D. J. Wilson
College of Optical Sciences, University of Arizona, Tucson, Arizona 85721, USA

CONTENTS

I. MEMBRANE FABRICATION

Patterned and unpatterned membrane samples are fabricated on the same 100 mm wafer. Stoichiometric, high stress Si_3N_4 is grown by low pressure chemical vapor deposition (LPCVD) on both sides of a 200 µm-thick silicon wafer. The initial deposition stress is estimated a posteriori from the observation of membrane resonant frequencies, and varies in the range 900-1100 MPa, changing slightly with deposition run.

The fabrication process relies on bulk wet etching of silicon in KOH through the whole wafer thickness, to create openings for optical access to the membranes samples [1–4]. The extremely high selectivity of Si_3N_4 to Si during KOH etching allows the use of the backside nitride layer as a mask, to define the outline of the membranes on the frontside.

Initially, the frontside nitride (Si_3N_4) layer is patterned with h-line photolithography and CHF_3/SF_6-based reactive ion etching (RIE) (steps 2-3 of figure S1). The photoresist film is then stripped with a sequence of hot N-Methyl-2-pyrrolidone (NMP) and O_2 plasma; this procedure is carefully repeated after each etching step. The frontside nitride layer is then protected by spinning a thick layer of negative-tone photoresist (MicroChemicals AZ®15nXT), prior to flipping the wafer and beginning the patterning of membrane windows on the backside nitride layer (steps 4-5). We noticed a reduction in the occurrence of local defects and increased overall membrane yield when the unreleased membranes on the frontside were protected from contact with hot plates, spin-coaters and plasma etchers chucks. The backside layer is then patterned with membrane windows, in a completely analogous way. The exposure step requires a wafer thickness-dependent rescaling of membrane windows, to account for the slope of slow-etching planes in KOH, and careful alignment with frontside features.

After stripping the photoresist, the wafer is installed in a PTFE holder for the first wet etching step in KOH at $\approx 75\,^{\circ}C$ (step 6). The holder clamps the wafer along its rim, sealing off the wafer frontside with a rubber O-ring, while exposing the backside to chemical etching by KOH. This procedure is necessary to ensure that PnC membranes are suspended correctly: we noticed that releasing PnC samples by etching from both sides of the wafer produced a large number of defects in the phononic crystal, probably due to the particular dynamics of undercut and stress

* These authors contributed equally
† tobias.kippenberg@epfl.ch

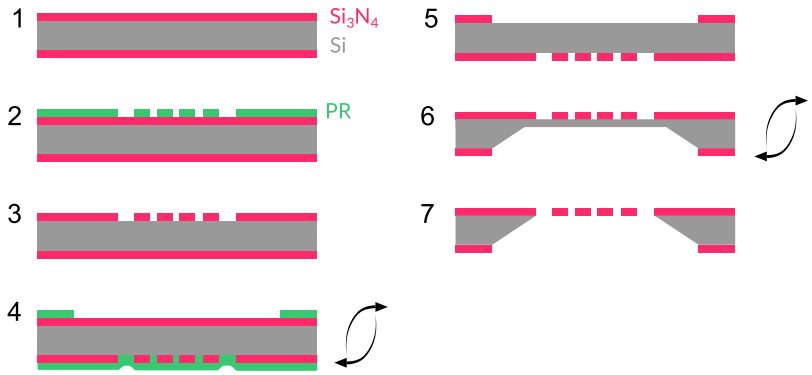

Figure S1. Main steps of the fabrication process. Magenta - Si_3N_4; gray - Si; green - photoresist.

relaxation in the film. The wafer is etched until 30-40 µm of silicon remains, leaving the samples robust during the subsequent fabrication steps. The wafer is then removed from the KOH bath and the PTFE holder, rinsed and cleaned in concentrated HCl at room temperature for 2 hours [5].

Subsequently, the wafer is coated with thick, protective photoresist and diced into 8.75 mm × 8.75 mm chips, and the remainder of the process is carried on chip-wise. Chips are cleaned again with hot solvents and O_2 plasma, and the membrane release is completed by exposing chips to KOH from both sides (step 7). The temperature of the solution is lowered ($\approx 55 - 60\,^{\circ}\mathrm{C}$), to mitigate the perturbation of fragile samples by buoyant N_2 bubbles, a byproduct of the etching reaction. After the undercut is complete, the samples are carefully rinsed, cleaned in HCl, transferred to an ethanol bath and gently dried in a critical point dryer (CPD).

II. QUADRATIC MECHANICAL DISPLACEMENT TRANSDUCTION BY THE OPTICAL CAVITY VERSUS QUADRATIC OPTOMECHANICAL COUPLING

Nonlinear cavity transduction can produce signals, quadratic in mechanic displacement, that are orders of magnitude stronger than those due $\partial^2\omega_c/\partial x^2$ terms that were ever experimentally demonstrated[**?**]. Below we derive the classical dynamics of optical field in an optomechanical cavity taking into account terms that are quadratic in displacement. We show that in membrane in the middle cavity typical quadratic signals originating from the nonlinear transduction are $r\mathcal{F}$ larger than the signals due to the nonlinear optomechanical coupling, $\partial^2\omega_c/\partial x^2$.

The fluctuations of ν due to the mechanical displacement are given by

$$\delta\nu(t) \approx 2\frac{G}{\kappa}x(t) + \frac{G_2}{\kappa}x(t)^2, \tag{S1}$$

where $G = -\partial\omega_c/\partial x$ and $G_2 = -\partial^2\omega_c/\partial^2 x$ are the linear and quadratic optomechanical coupling, respectively, and the total displacement x is composed by partial contributions of different modes x_n

$$x(t) = \sum_n x_n(t). \tag{S2}$$

For resonant lase probe we can find the intracavity field as

$$a(t) \approx 2\sqrt{\frac{\eta_1}{\kappa}}(1 - i\nu(t) - \nu(t)^2)s_{\mathrm{in},1} = 2\sqrt{\frac{\eta_1}{\kappa}}\left(1 - 2i\frac{G}{\kappa}x(t) - \left(\left(2\frac{G}{\kappa}\right)^2 + i\frac{G_2}{\kappa}\right)x(t)^2\right)s_{\mathrm{in},1}. \tag{S3}$$

It is instructive to compare the magnitudes of the two contributions to the prefactor of $x(t)^2$. The typical value for G (assuming the membrane to be not very close to one of the mirrors) is

$$G \sim 2r\frac{\omega_c}{l_c}, \tag{S4}$$

while the typical value for G_2 is[**?**]

$$G_2 \sim 4\frac{r\omega_c^2}{c\,l_c}, \tag{S5}$$

where c is the speed of light, r is the membrane reflectivity and l_c is the cavity length. The ratio of the two contributions is evaluated as

$$\left(2\frac{G}{\kappa}\right)^2 \Big/ \left(\frac{G_2}{\kappa}\right) \sim \mathcal{F}r. \tag{S6}$$

As the cavity finesse $\mathcal{F}$ is typically large, on on the order of 10^3 to 10^5, and the membrane reflectivity r is between 0.1 and 0.5, we conclude that linear optomechanical coupling needs to extremely well suppressed in order for the quadratic coupling G_2 to contribute.

III. DISSIPATIVE COUPLING

In an optomechanical membrane-in-the-middle cavity dissipative coupling, $\partial\kappa/\partial x$, exists in addition to the dispersive coupling, $\partial\omega_c/\partial x$. Dissipative coupling modulates the optical decay rate, both external coupling and intrinsic loss, and potentially can produce intensity noise in a resonantly locked probe laser. However, for the parameters of our experiment the dissipative coupling is negligible.

The noise due to dissipative coupling can be upper-bound as follows. The cavity linewidth cannot change by more than κ as the membrane is translated by λ inside the cavity, and therefore the dissipative coupling rate is limited by

$$\frac{\partial\kappa}{\partial x} \lesssim \frac{\kappa}{\lambda} = \frac{1}{\mathcal{F}}\frac{\omega_c}{2l_c} \sim \frac{G}{\mathcal{F}}, \tag{S7}$$

where in the last transition it was assumed that the membrane reflectivity is not very much smaller than one.

Resonant intracavity field modulated by dissipative coupling only is given by

$$a(t) \approx 2\sqrt{\frac{\eta_1}{\kappa}}\left(1 - \frac{1}{2\kappa}\frac{\partial\kappa}{\partial x}x(t)\right)s_{\mathrm{in},1}. \tag{S8}$$

Comparing to Eq. S3, we find that the noise produced by dissipative coupling is negligible compared to the intermodulation noise if

$$\frac{G}{\kappa}x \gg \frac{1}{\mathcal{F}}. \tag{S9}$$

In all the experiments presented in this work this condition is satisfied, Gx/κ ranges from 0.1 to 0.01 [verify exact numbers], whereas $1/\mathcal{F}$ is always less than 10^{-4}.

IV. LASER AND MIRROR NOISES

Here we present the measurements of amplitude noise of TiSa laser plus the frequency noise noise of an empty Fabry-Perot cavity.

V. DETAILS OF THE TIN CALCULATIONS

VI. MODEL OF TIN IN PRESENCE OF DYNAMICAL BACKACTION COOLING

[1] Y. Tsaturyan, A. Barg, E. S. Polzik, and A. Schliesser, Nature Nanotechnology **12**, 776 (2017).
[2] C. Reinhardt, T. Müller, A. Bourassa, and J. C. Sankey, Physical Review X **6**, 021001 (2016).
[3] R. A. Norte, J. P. Moura, and S. Gröblacher, Physical Review Letters **116**, 147202 (2016).
[4] C. Gartner, J. P. Moura, W. Haaxman, R. A. Norte, and S. Groblacher, Nano Letters **18**, 7171 (2018).
[5] C. B. Nielsen, C. Christensen, C. Pedersen, and E. V. Thomsen, Journal of The Electrochemical Society **151**, G338 (2004).